AUTOMATIC DETECTING DISBONDS IN LAYERED STRUCTURES USING ULTRASONIC PULSE-ECHO INSPECTION

Tadeusz Stepinski and Bengt Vagnhammar, Uppsala University, Signals and Systems, Box 528, SE-751 20 Uppsala, Sweden

(To appear in Proceedings of the 7th ECNDT)

Abstract

A method for automatic detection of disbonds in layered structures based on time-frequency representation of the ultrasonic signals acquired during ultrasonic inspection is presented in the paper. The detection is performed by a multilayer perceptron neural network using features extracted from the time-frequency representation as inputs. The performance of the detector is demonstrated using data from the pulse-echo inspection of a multilayered aerospace structure covered with rubber.

Introduction

Inspection of layered structures using pulse-echo ultrasound is a classical NDT method used in the aerospace industry. Detection of disbonds between different layers is possible due to the change of reflection coefficient resulting in variations of amplitude and phase of the respective echoes. In some practical applications where the ultrasonic coupling is not reliable and/or the damping in the upper layer is variable, the phase information is more reliable for the detection than the amplitude of the echo.

The main problem encountered in this type of inspection is narrow band characteristics of the measurement system, especially ultrasonic transducer. The pulses reflected from the interfaces between layers are filtered by the transducer used in the test. Since it is difficult to construct a transducer with sufficiently short impulse response the pulse train received from the structure is ”smeared” by the transducer which makes detecting disbonds very difficult or even impossible.

Our main objective was developing a signal processing technique capable of detecting disbonds at the adhesive interface between isolation rubber and aluminum based on pulse-echo ultrasound data. Pulse-echo was to be used since only one side of the object will is accessible in the real test situation. The two main inspected structures were: thick rubber layer on aluminum plate "Plate" and thick rubber layer on honeycomb "Honeycomb" (see Figure 3 and 4 for details).

A first idea, when looking at signals coming from test object "Plate", is that automatic classification should be possible just by detecting the plate "ringing" following the main echo (cf Figure 5, 6 and 7). It appeared however, that these "ringings" were not be very reliable at all, especially if the measurements were corrupted by noise. Phase information is also difficult to use in the time-domain where the appearance of the echo can change with a varying layer

thickness. Therefore, we have developed a simple time-frequency representation of the signal capable of extracting relatively robust features for the detection.

Since the main goal was to automatically inspect and detect defect areas, a decision had to be made whether the signal comes from a flaw or not. The detection, or detecting decision, was made by a neural network classifier using features extracted from each measured signal. With feature vectors in a low-dimensional feature space we obtained good representation of the data distribution (within these dimensions) even for relatively few measurements.

Signal representation

Since we are dealing with close located pulses convoluted with a long transducer impulse response we encounter interference phenomena and classical Fourier analysis appears to be inappropriate tool for feature extraction in this case. The signal is nonstationary and the amplitude spectrum does not provide the relevant information about it. If we encounter in the signal both constructive and destructive interference for the same frequency at different time instances, they will tend to cancel the effect of each other. We have to study frequency variations between time intervals (windows) comparable in size with two times the travel time in the layer of interest. Since we do not know exactly where in the signal the interesting interval will be found, we use a time-frequency representation of our signal.

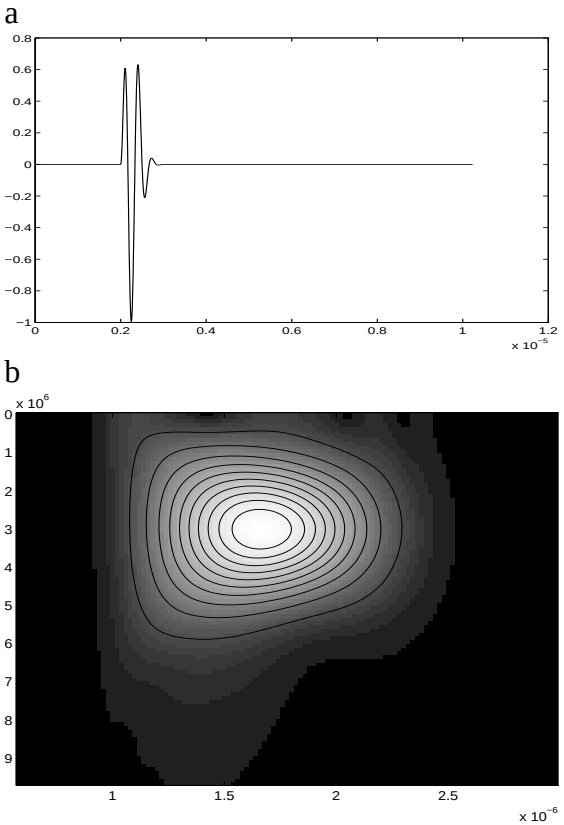

Figure 1. Single pulse (a) and its time-frequency representation (b). Time in μs on the horizontal axis and frequency in MHz on the vertical axis.

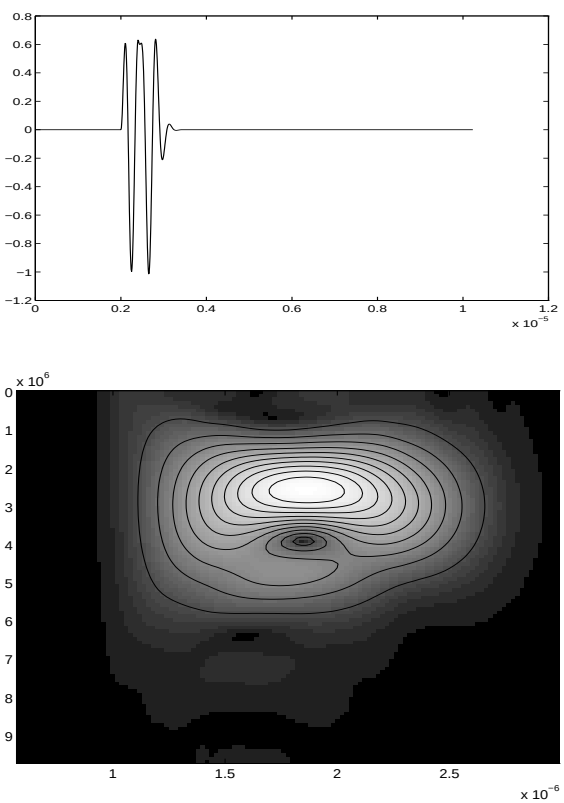

Figure 2 Two pulses (a) and their time-frequency representation (b). Time in μs on the horizontal axis and frequency in MHz on the vertical axis.

By windowing the signal, to contain just one multiple reflection within a layer, destructive interference should occur for some frequency, and hopefully within the frequency band excited by the transducer. We can illustrate this with a simple one-dimensional linear model.

If we have one (or two) interfaces reflecting energy, the material response will take the form of one (or two) delayed Dirac pulses. After convoluting the material response with the transducer prototype we get a simulation of a hypothetical measurement (see Figure 1a and 2a). Using a window that is shifted along the time-scale, and calculating a zero-padded FFT for its each position, we can generate images like those in Figure 1b and 2b constructed by putting all resulting spectra next to each other in columns.

In Figures 1 and 2, the transducer prototype had a center frequency of 3.5 MHz and a bandwidth of 1.5 MHz. The convoluted signal vector had 1024 samples sampled with an interval of 10 ns (corresponding to sampling frequency 100 MHz). Each column in the time-frequency representation is the amplitude spectrum of the windowed signal using a 124 samples wide Hanning window. In Figure 2a the two Dirac pulses are separated by 40 samples. We should then have constructive interference at 100 MHz/40 = 2.5 MHz, and destructive interference at 100/40*3/2 MHz = 3.75 MHz. This has the effect that the peak found at 3 MHz in Figure 1b (left) is pulled towards 2.5 MHz, and at the same time pushed away from the dip at 3.75 MHz. This simple example illustrates how the presence of disbond is indicated by presence of a frequency dip in the time-frequency representation of the signal. This appears to work also for real signals as illustrated in Figure 5 below.

Experiments

The test objects used in this project were made available through CSM Materialteknik AB, who also performed all measurements used in this report. Two different structures were manufactured to serve as test objects. The first was rubber on aluminum plate (see Fig. 3 below), and the second was rubber on honeycomb (see Fig. 4 below). Flaws were included to simulate the presence of upper and lower interface disbonds in the glue layer.

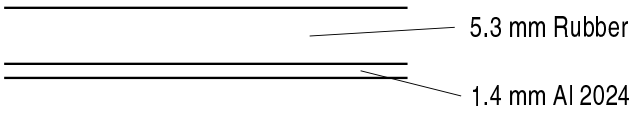

Figure 3. Test object "Plate" consisting of rubber glued to an aluminum plate.

The second object is a bit more complex. Under the aluminum plate, which is thinner, there is a honeycomb structure. It can capture and scatter ultrasonic energy, and the signal could be expected to change a little depending on where on the hexagon grid the transducer is positioned. There is also an aluminum plate on the backside, but the objective in this project has been to detect disbonds in the first adhesive layer where the same flaws exist as for object "Plate". The artificial disbonds were manufactured in sizes (in mm): 30x30, 20x20 and 10x10.

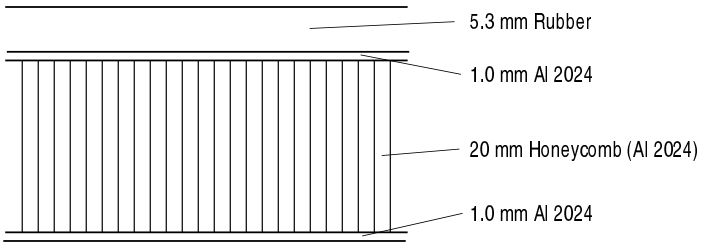

Figure 4. Test object "Sandwich" consisting of rubber glued to a honeycomb structure.

The signals obtained during pulse-echo inspection of the above samples using an ultrasonic instrument (Krautkrämer USD 15) and an application specific 5MHz transducer are shown in

Figures 5, 6 and 7. From the figures can be seen that the signals measured for the structures with disbonds can be relatively easily distinguished from those obtained for defect free structures. However, the classification of the disbond (upper or lower) is more difficult. Even detecting disbonds can be difficult in practical situations where the ultrasonic signals are corrupted by noise or the disbond is not distinct.

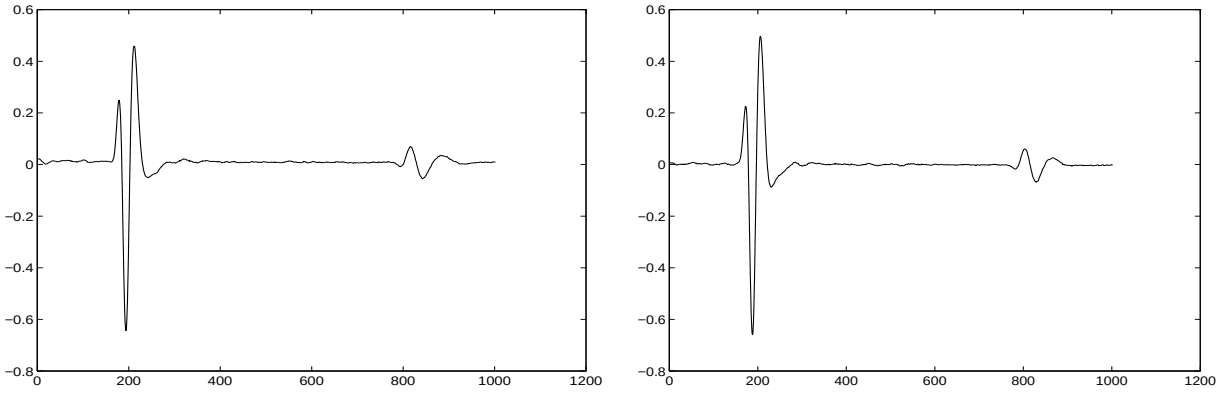

Figure 5. Samples from objects “Plate” (left) and “Honeycomb” (right) containing upper disbonds.

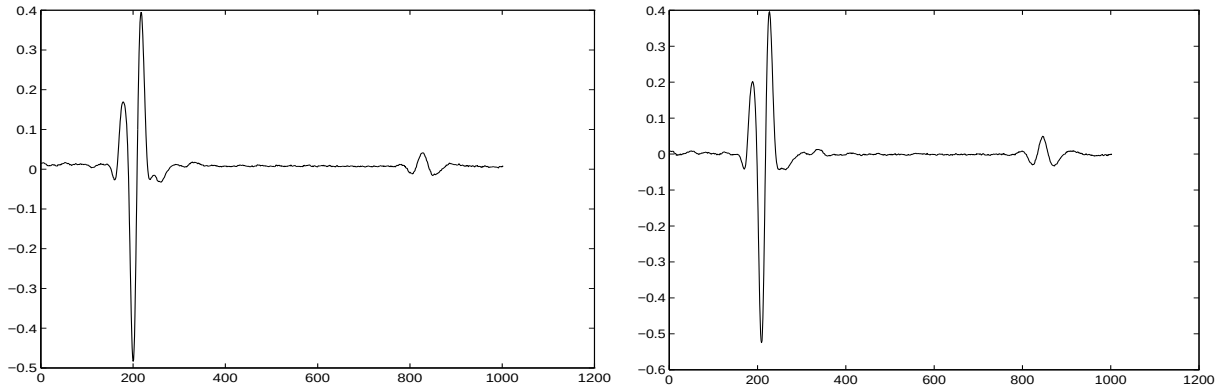

Figure 6. Samples from objects “Plate” (left) and “Honeycomb” (right) containing lower disbonds.

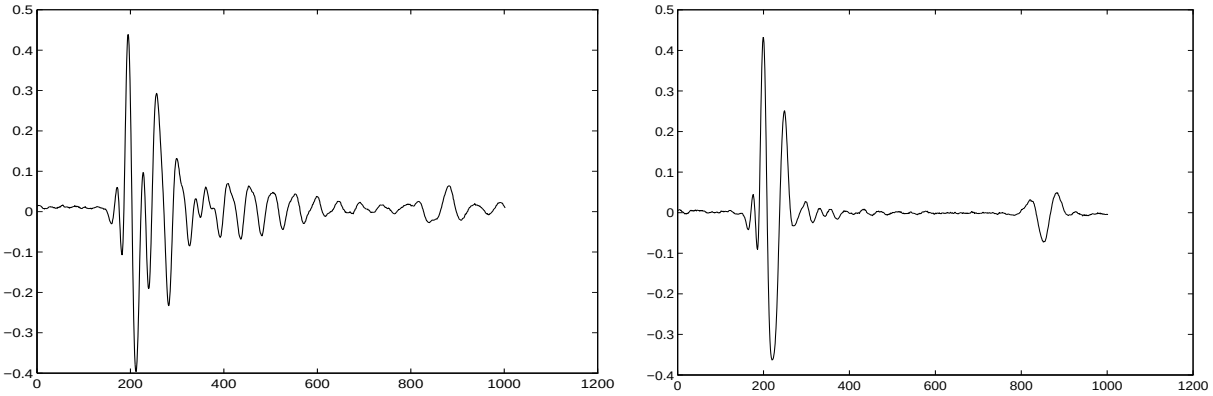

Figure 7. Samples from defect free objects “Plate” (left) and “Honeycomb” (right).

The signals presented in Figures 5 to 7 were subjected to windowing, zero-padding, normalization and finally time frequency transformation (see [1] for details). From their time-frequency representation, shown in Figure 9, and from the analysis of other signals can be

seen that the defect-free bounds have a characteristic dip in the time-frequency representation. Therefore features determining presence of the dip can be used for the classification.

Feature extraction was performed in two steps, first a rectangular window (region of interest, ROI) where the frequency deep occurred was selected, and than two features (curvature feature and gradient feature) characterizing shape of the surface in the ROI were calculated.

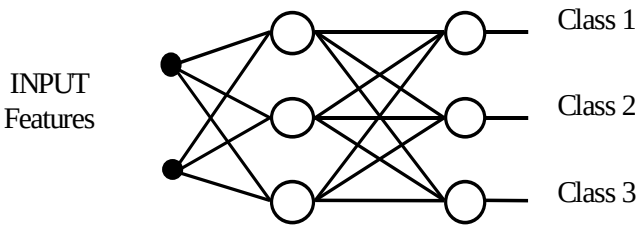

Figure 8. Neural Network structure with three hidden and three output nodes used for the classification.

These features were used as inputs to a simple multi-layer perceptron with 2 inputs, 3 hidden nodes and 3 outputs (see figure 8). Each output node corresponded to one class, defect-free, upper delamination, and lower delamination..

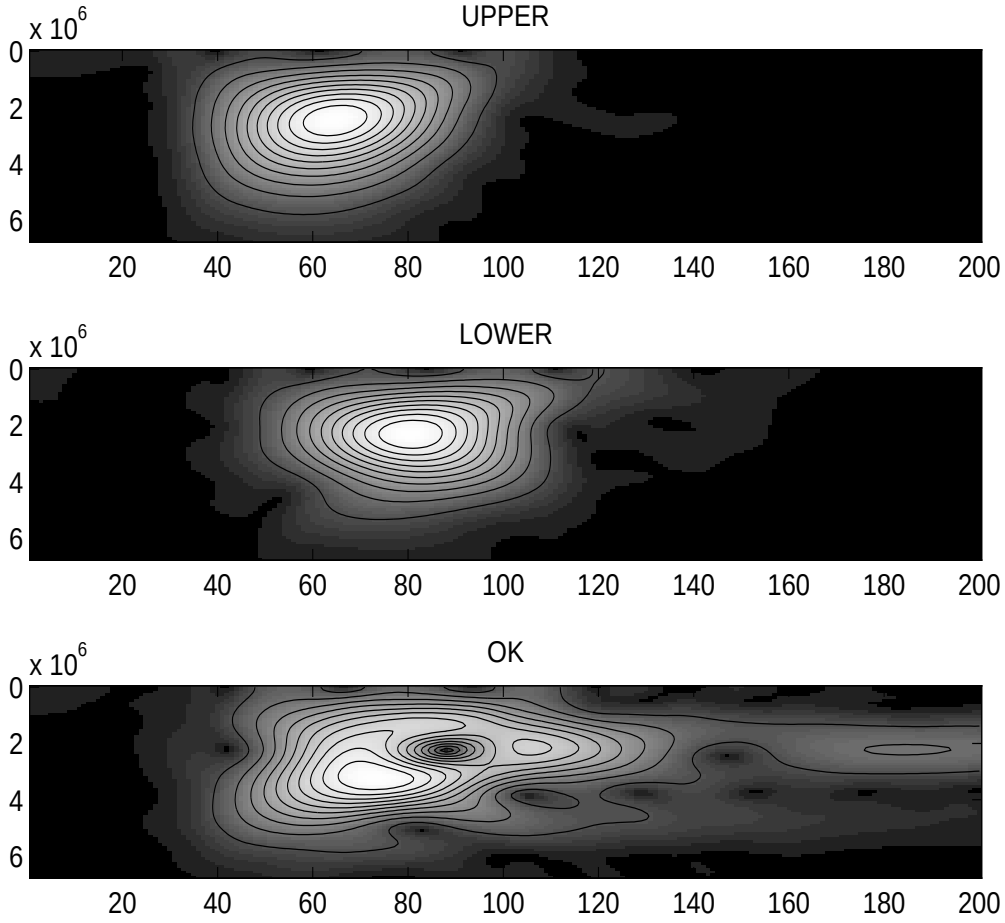

Figure 9. Time frequency representations of three measured signals. Disbond in upper layer (upper), disbond in the lower layer (middle) and a defect-free structure (bottom). Arbitrary units on axies.

Training was performed on labeled data and the output nodes were encouraged to output a one if features from their class are presented to the classifier, and zero otherwise. This method in combination with the training algorithm would make the output values approximate the a posteriori probabilities [3]. The decision consisted then in taking the most probable class given the input presented, i.e., classifying the pattern as the output node with the highest value

To verify the performance of the classifier, "leave-one-out" training was used. Each class member was left out of training once. The trained classifier was then applied to this example not having been seen during the training. Training was allowed to continue until the error was below 10^{-2}. The results presented in table 1 show that the classification was correct for all the "leave-one-out" classes..

Table 1. Correct classifications (total number of patterns) and performance measured as total fraction of correct classifications

Object	Upper	Lower	Ok	Performance
"Plate"	7 (7)	7 (7)	10 (10)	100 %
"Honeycomb"	7 (7)	7 (7)	11 (11)	100 %

Performance of the classifier was evaluated in a blind test using 100 real measurements performed on a rubber lined plate and a honeycomb structure (the data was provided by CSM Materialteknik AB). According to CSM who evaluated the results the classifications were 100% correct, which means that all disbonds were detected and classified correctly

Conclusion

In this paper a method suitable for automatic detection of disbonds based on time-frequency representation of the ultrasonic signals acquired during the inspection of layered structures was presented. The time-frequency representation serves as a preprocessing method enabling extraction of features used for the detection. The features are amplitude invariant and robust against changes of the inspection parameters, such as, ultrasonic coupling and acoustic impedance of the layer under the disbond area.

The features extracted from the time-frequency representation are fed to a multilayer perceptron neural network performing the detection. The time-frequency representation of the signal presented here yields features good enough for transforming the difficult time domain classification issue into a relatively simple task. This was confirmed by the outstanding 100 % correct classification in the blind test. It is shown that in this case the detector is capable of detecting very small (10 x 10 mm) artificially introduced disbonds for two different types of structures, aluminum plate and honeycomb structure lined with gum.

Simulations made also indicate that the method is relatively insensitive to changes in thickness in the rubber and the epoxy layer. This is imperative, especially since the epoxy layer can vary considerably from one point to another. The property of being robust against added noise indicates that the method could be applied to a measuring device using a water jet. The possibility of automation therefore seems promising. The classification itself can easily be made automatic.

Acknowledgments. This study was funded by the Swedish National Flight Research Program (NFFP) in project NFFP-274. The author would acknowledge the assistance of Bertil Grelsson from CSM Materialteknik AB for performing the ultrasonic measurements.

References

1. Vagnhammar B, L Ericsson, T Stepinski and B Grelsson, Improved defect detection in ultrasonic inspection of bonded structures, Report UPTEC 97 105R, Uppsala University, June, 1997
2. Munns IJ, GA Georgiou, "Non-destructive testing methods for adhesively bonded joint inspection - a review", INSIGHT, Vol 37, No 12, Dec 1995, pp 941-952
3. Callis RE, RJ Freemantle, JDH White an GP Wilkinson, Ultrasonic compression wave NDT of adhered metal lap joints of uncertain dimensions, INSIGHT, vol 37, no 12, 1995, pp. 954-963.
4. Michael D R, R P Lippmann, Neural Network Classifiers Estimate Bayesian a posteriori Probabilities, NEURAL COMPUTATIONS 3, 1991, pp 461-483